

## Research Article

# Determination of Adsorption of Methylene Blue Dye by Incense Stick Ash Waste and Its Toxicity on RTG-2 Cells

**Virendra Kumar Yadav,<sup>1,2</sup> Nisha Choudhary<sup>3</sup>, Daoud Ali,<sup>4</sup> Gokhlesh Kumar,<sup>5</sup> G. Gnanamoorthy<sup>6</sup>, Azhar Ulla Khan,<sup>7</sup> Pankaj Kumar<sup>8</sup>, S. Hari Kumar,<sup>9</sup> and Belachew Zegale Tizazu<sup>10,11</sup>**

<sup>1</sup>Department of Microbiology, School of Sciences, P P Savani University, Surat, 394315 Gujarat, India

<sup>2</sup>Department of Microbiology, School of Liberal Arts & Sciences, Mody University, Laxmangarh, Sikar, 332311 Rajasthan, India

<sup>3</sup>Department of Environment Sciences, School of Sciences, P. P. Savani University, Surat, 394315 Gujarat, India

<sup>4</sup>Department of Zoology, College of Science, King Saud University, PO Box 2455, Riyadh 11451, Saudi Arabia

<sup>5</sup>Clinical Division of Fish Medicine, University of Veterinary Medicine Vienna, 1210 Vienna, Austria

<sup>6</sup>Department of Inorganic Chemistry, University of Madras, Guindy Campus, Chennai, Tamil Nadu, India

<sup>7</sup>School of Basic and Life Sciences, Jaipur National University, Jaipur, Rajasthan, India

<sup>8</sup>Integrated Regional Office, Ministry of Environment, Forest and Climate Change (MoEFCC), Government of India, Saifabad, Hyderabad 500004, India

<sup>9</sup>Department of Chemistry, Rajalakshmi Institute of technology, Kuthambakkam, Chennai 600124, India

<sup>10</sup>Center of Excellence for Bioprocess and Biotechnology, Addis Ababa Science and Technology University, Ethiopia

<sup>11</sup>Department of Chemical Engineering, College of Biological and Chemical Engineering, Addis Ababa Science and Technology University, Ethiopia

Correspondence should be addressed to Belachew Zegale Tizazu; [belachew.zegale@aastu.edu.et](mailto:belachew.zegale@aastu.edu.et)

Received 15 March 2022; Revised 13 April 2022; Accepted 5 May 2022; Published 21 May 2022

Academic Editor: Lakshmiopathy R

Copyright © 2022 Virendra Kumar Yadav et al. This is an open access article distributed under the Creative Commons Attribution License, which permits unrestricted use, distribution, and reproduction in any medium, provided the original work is properly cited.

Incense stick ash (ISA) has traces of toxic heavy metals which have an adverse effect on the environment. Every year, tonnes of ISA are disposed of in rivers and other water bodies which leads to water pollution and affects the natural water resources. ISA has several value-added minerals which could be modified or functionalized for environmental cleanup. Here, in the current research work, ISA was transformed into a flower-like noble porous material by mixing ISA and NaOH in a 1 : 1 ratio followed by calcination at 600°C for six hours in a muffle furnace. The developed material was analyzed by sophisticated instruments for the identification of the properties. The microscopic techniques revealed the micron-sized flower-like structure, while the XRD showed peaks at 30–33° which indicates the transformation of the calcite and silicate phases into new-phase mineral. FTIR also revealed bands in regions of 500–1200 cm<sup>-1</sup> and new bands near 450 cm<sup>-1</sup>. EDS confirmed the presence of Na in the sintered product and the transformation of the ISA. Finally, the sintered product potential was assayed for the removal of methylene blue dye from wastewater using an adsorption mechanism. The removal efficiency of dye reached up to 70% within one hour only. It was found that the ISA sintered product has the potential to remove MB dye efficiently from wastewater and also reduce solid waste pollution. Microculture tetrazolium assay (MTT) and lactate dehydrogenase (LDH) assays were performed to evaluate the cytotoxicity of the sintered incense stick ash product on RTG-2 cells. The sintered incense stick ash product induced cytotoxicity on RTG-2 cells in a dose-dependent manner. Sintered ISA products have the potential to remove methylene blue dye efficiently from wastewater and reduce solid waste pollution.

TABLE 1: Concentration of heavy metals and other trace elements in the incense stick ash analyzed by inductively coupled plasma-optical emission spectroscopy (ICP-OES), adopted from [11].

Elements	Conc (ppm)
Be	0.10
Ca	195.8
Cr	1.771
Cd	0.002
Co	0.305
Cu	3.602
Fe	378.0
Li	0.259
Mg	323.4
Mn	24.98
Mo	0.056
Ni	1.284
Pb	0.156
Sb	0.164
Se	0.014
Sr	5.327
Ti	24.86
V	0.378
Zn	2.825

TABLE 2: Major elemental oxides present in the ISA analyzed by X-ray fluorescence adopted from [11].

Elements	Wt %
SiO <sub>2</sub>	20.362
Al <sub>2</sub> O <sub>3</sub>	4.775
P <sub>2</sub> O <sub>5</sub>	3.946
SO <sub>3</sub>	3.776
Na <sub>2</sub> O	0.097
MgO	3.915
K <sub>2</sub> O	8.247
CaO	49.616
TiO <sub>2</sub>	0.609
MnO <sub>2</sub>	0.158
Fe <sub>2</sub> O <sub>3</sub>	4.288
CuO	0.087
SrO	0.120
Total	99.996

## 1. Introduction

Our natural resources are continuously depleted by various organic and inorganic pollutants [1]. There are several inorganic pollutants like heavy metals, while there are organic pollutants like pesticides, microbes, and dyes. Every year, huge amounts of dyes from various industries are discharged into rivers or other water bodies which leads to water pollution by affecting the flora and fauna [2]. One such dye is methylene blue (C<sub>16</sub>H<sub>18</sub>ClN<sub>3</sub>S (MB)) [3], which

is a cationic dye and is most frequently used as chemical indicators, dyes, and biological stains [3]. It is considered carcinogenic after a certain level so it requires immediate attention. The wastewater or water bodies loaded with methylene blue (MB) have high chromaticity, high organic matter, and less biodegradability which ultimately leads to harmful effects on the health of humans and animals. The major sources of MB pollution in water are the dye industries and research laboratories. Earlier, numerous technologies (biological, chemical, and physical) have been applied by several investigators from time to time to remove MB from wastewater. The most widely used traditional approaches are photocatalytic degradation [4], precipitation, coagulation, flocculation, ozonation, membrane filtration, advanced oxidation, and biodegradation [3]. Most of these conventional methods have limitations, due to the complex and expensive approaches. So, there is a requirement for a reliable, economical, and easy approach for the remediation of MB dye from wastewater. Among all the available dye removal techniques, the adsorption-based technique is most preferred due to its simpler and economical nature, high efficiency, and insensitivity to toxic substances [3]. One of the major factors that make the adsorption process very economical is the cost of the adsorbent [5]. If the adsorbent is derived from an economical product or by-products, then, the adsorption or removal of MB dye will become economical. Though nanobased techniques are quite effective at a much lesser dosage [6], the expensive precursors, synthesis techniques, and analysis methods make the nano-adsorption unfeasible. The commonly used nano-adsorbents like nanosilica, titania, zinc oxide, and iron oxide are quite expensive due to the above-mentioned factors [7, 8]. So, it is time to switch to the new material or by-products for the adsorption of the dye from wastewater. One such highly underestimated material is incense sticks ash (ISA), which is the residual product of incense sticks generated after combustion at religious places and houses. India secures 4th position in exporting incense sticks and 3rd position in consumption of incense sticks [9, 10]. The black-colored incense sticks have coal or charcoal powder, as a burning agent for the incense sticks [4]. Coals contain a high level of toxic heavy metals like, Cd, Hg, Cu, Ni, Co, Cr, Mo, Zn, and As (shown below in Table 1) and several value-added minerals like calcium oxides and carbonates, ferrous, silica, alumina, and carbon (shown in Table 2). So, here, the authors have used incense stick ash waste as a raw material for the adsorption process after surface modification or alkali activation by NaOH followed by sintering.

In the current research work, the authors have focused on the synthesis of incense stick ash-derived value-added products like the ISA-NaOH sintered product. Firstly, ISA was mixed with fine pellets of NaOH in a quartz crucible. Further, the mixture was mixed thoroughly and calcinated at 600°C for six hours to obtain the porous-sintered product. The instrumental analysis revealed that the synthesized sintered products are flowers, micron sized, i.e., 100 nm to 9 microns. Finally, the ISA-NaOH porous sintered product was assessed for their property towards the remediation of

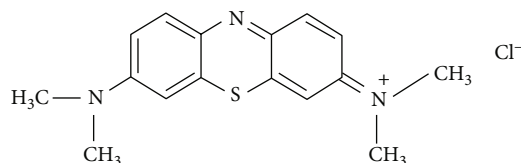


FIGURE 1: Chemical structure of methylene blue dye.

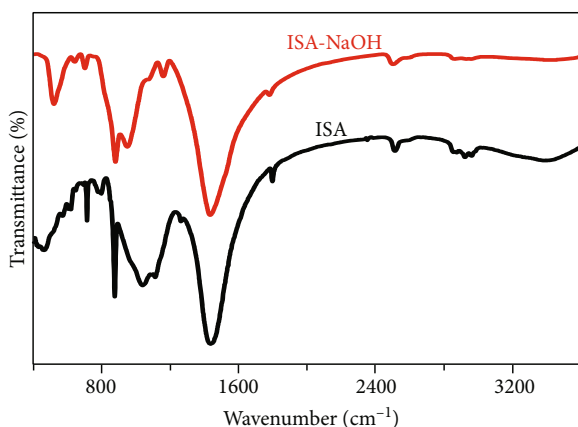


FIGURE 2: FTIR spectra of ISA and sintered product.

methylene blue dye from the aqueous solution while, cytotoxicity was assessed on RTG-2 cells.

## 2. Materials and Analysis

**2.1. Chemical and Reagents.** MTT [3-(4, 5-dimethylthiazol-2-yl)-2, 5-diphenyltetrazolium bromide] was purchased from Sigma-Aldrich (St. Louis, Missouri, United States). Dulbecco's modified Eagle's medium (DMEM), fetal bovine serum (FBS), and antibiotics were purchased from Gibco, USA.

MB dye was procured from Molychem, India, whose structure is shown in Figure 1. ISA was collected from the Uttam Nagar temple, New Delhi, India. NaOH was purchased from RENKEM, India. Nickel crucible was used to place the samples in a muffle furnace.

The collected ISA was screened in the laboratory, by using sieve sets, to eliminate the unburned particles, bamboo sticks, and other undesired products.

**2.2. Formation of the Sintered Product from Incense Stick Ash.** About 50 grams of ISA was taken in a nickel crucible, and about 20 grams of NaOH pellets was added and mixed properly by using a glass rod for even distribution. Further, the crucible containing the mixture was placed in a muffle furnace by gradually increasing the temperature, 10°C per 5 minutes till the temperature reached 600°C. Once the temperature reached 600°C, the calcination was carried out for 6 hours. After calcination was over, the crucible was placed in a desiccator. Further, the lumped product was crushed to powder by using a mortar and pestle. Finally, the obtained product was analyzed by the Fourier transform infrared spectroscopy (FTIR) (Spectra SP65, PerkinElmer, Germany), X-ray diffraction (XRD) (Bruker, D8 Advance), field emis-

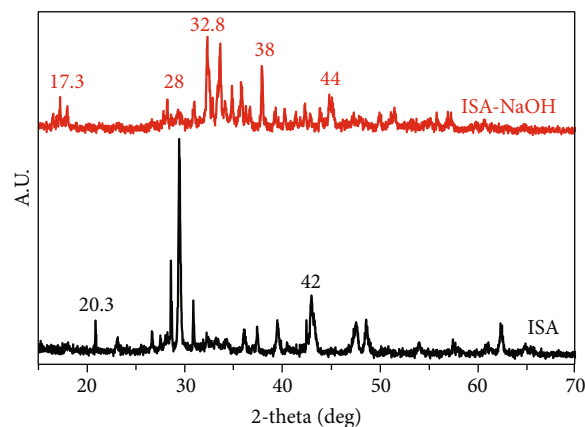


FIGURE 3: XRD diffract graph of ISA and sintered product.

sion scanning electron microscopy (FESEM) (Nova Nano-SEM 450), and energy dispersive spectroscopy (EDS) (Bruker) for the detailed morphological and elemental properties.

**2.3. Adsorption Study of Methylene Blue.** The experiments of batch adsorption were carried out in a thermostatically controlled shaker with Erlenmeyer flasks. The effect of parameters on the time was tested on the efficiency of adsorption. A 200 ppm of MB dye solution was prepared by dissolving 20 mg of MB dye which was dissolved in 100 mL of distilled water. About 20 mg of sintered ISA was added to the 50 mL of dye solution. The mixtures were stirred for 60 minutes, and a 5 mL reaction mixture was extracted at a regular interval of 10 minutes. MB samples were removed from the shaker at present intervals of time and analyzed using a Halo DB-20, double-beam UV-Vis spectrophotometer (Dynamics). The percent dye decolorization and adsorption capacity of sintered ISA at any time ( $q_t$ ) were calculated using equation (1) as follows.

$$\% \text{decolorization} = \frac{A_0 - A_t}{A_0} \times 100, \quad (1)$$

$$q_t (\text{mg/g}) = \frac{(A_0 - A_t)V}{M},$$

where  $A_0$  is the initial MB concentration ( $\text{mg}\cdot\text{L}^{-1}$ ),  $A_t$  is the concentration of MB at a particular time ( $\text{mg}\cdot\text{L}^{-1}$ ),  $V$  is the volume of solution (liter), and  $M$  is the mass of sintered ISA (gm).

**2.4. Characterization.** The analysis of the sample was done by various sophisticated instruments. The functional group identification of ISA and the sintered product was done by the Fourier transform infrared spectroscopy (FTIR). About 2 mg ISA and sintered product was taken separately and mixed with 98 mg of a KBr spectroscopy grade. Both the samples were mixed thoroughly, and pellets were prepared, and measurement was done in the range of 400–4000  $\text{cm}^{-1}$  at a resolution of 1 nm by using a Model SP-65 (PerkinElmer) instrument. The minerals and phases of both ISA and the sintered product were analyzed by the X-ray diffraction

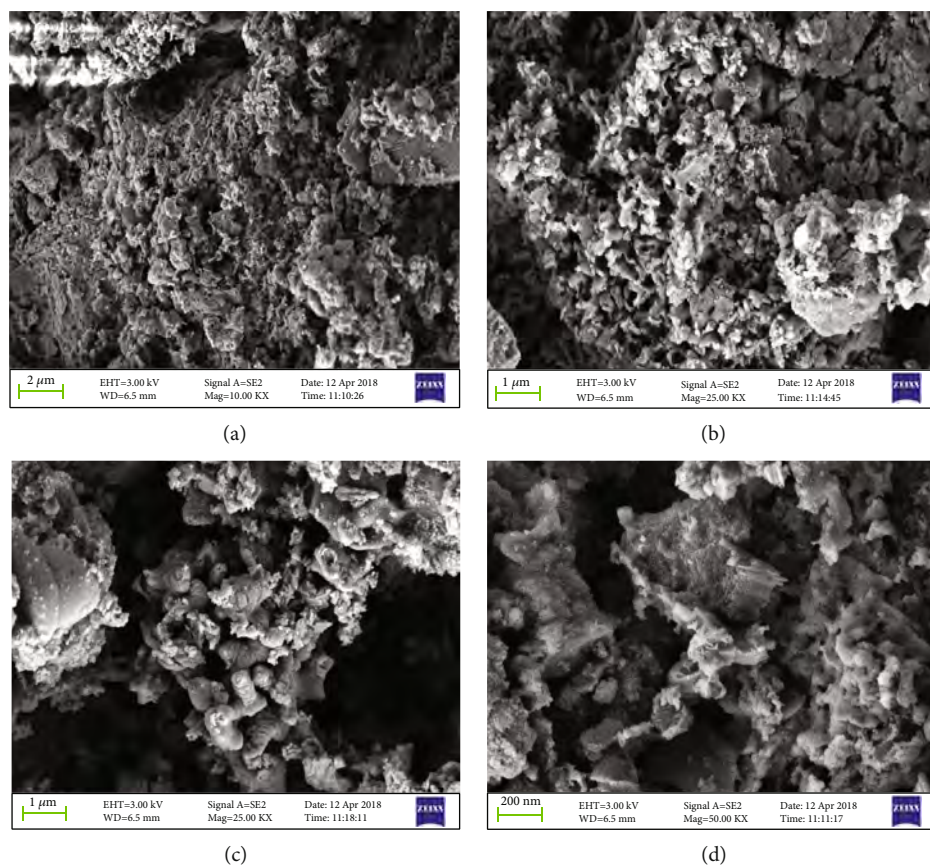


FIGURE 4: FESEM micrographs (a–d) of incense stick ash.

pattern (XRD). The measurement was done by a D8 Advance (Bruker) instrument in the range of 2 theta 0–80° with a step size of 0.02 and a time of 5 seconds per step at 40 kV voltage and a current of 30 mA. The morphology and size of both ISA and ISA sintered products were analyzed by the field emission scanning electron microscope, using NOVO NANOSEM, 450 (FEI, USA). For analysis, the powder sample was taken on a carbon tape, which was fixed on the aluminum stub. The sample along with the stub was placed in the gold sputtering chamber for gold coating. The sample was observed at different scales starting at 20 microns to 100 nm, while the elemental composition of ISA and the sintered product was detected by the Oxford-made, energy-dispersive spectroscopy attached with the FESEM. The remediation of MB in the aliquot was analyzed by the UV-Vis spectrophotometer Halo DB-20, double-beam UV-Vis spectrophotometer, (Dynamics) at a resolution of 1 nm.

**2.5. Cell Culture and Treatment of Incense Stick Ash.** The fish rainbow trout (*Oncorhynchus mykiss*) ovary (RTG-2) cell lines (90102529) were procured from Sigma-Aldrich Chemie GmbH, Eschenstrasse, 5D-82024, Taufkirchen. The cells were subcultured in EMEM (EBSS) + 2 mM glutamine + 1% nonessential amino acids (NEAA) + 10% fetal bovine serum (FBS) at a 5% CO<sub>2</sub> incubator at 24°C. The cells at 78% confluence were subcultured into 96-well plate cytotoxicity assay. RTG-2 cell lines were grown 24 h before treatment

to ISA. The stock solution of ISA was made in ddw and diluted according to the treatment concentrations (0–200 μg/mL). Control cells were not exposed to ISA and were considered as controls.

**2.6. MTT Assay.** The mitochondrial activity was determined by the MTT test (Cayman MTT assay kit). MTT solution (100 μL) was mixed with each well in a final concentration of 0.5 mg/mL and further left for incubation for 4 h. The formed formazan crystal was dissolved in DMSO, and the absorbance was determined at 570 nm using a microplate reader (BioTek Instruments, Winooski, VT, USA, equipped with Gen5 software, version 1.09).

**2.7. LDH Assay.** Leakage of lactate dehydrogenase enzyme, used as an indicator of cell membrane damage, was determined by LDH assay kit (Cytotoxicity Detection Kit, Roche Diagnostics, Milan, Italy) on the culture medium of cells exposed to 10, 50, 100, and 200 μg/mL of ISA for 24 h. Unexposed cells were used as a negative control. This colorimetric assay is based on the cleavage of a tetrazolium salt when LDH activity is present in the cell culture supernatant. The absorbance was measured at 490 nm using a spectrophotometric microtiter plate reader (BioTek Instruments, Winooski, VT, USA, equipped with Gen5 software, version 1.09).

**2.8. Statistical Analysis.** All statistical analyses were performed using SPSS 26.0 software (IBM). Differences were

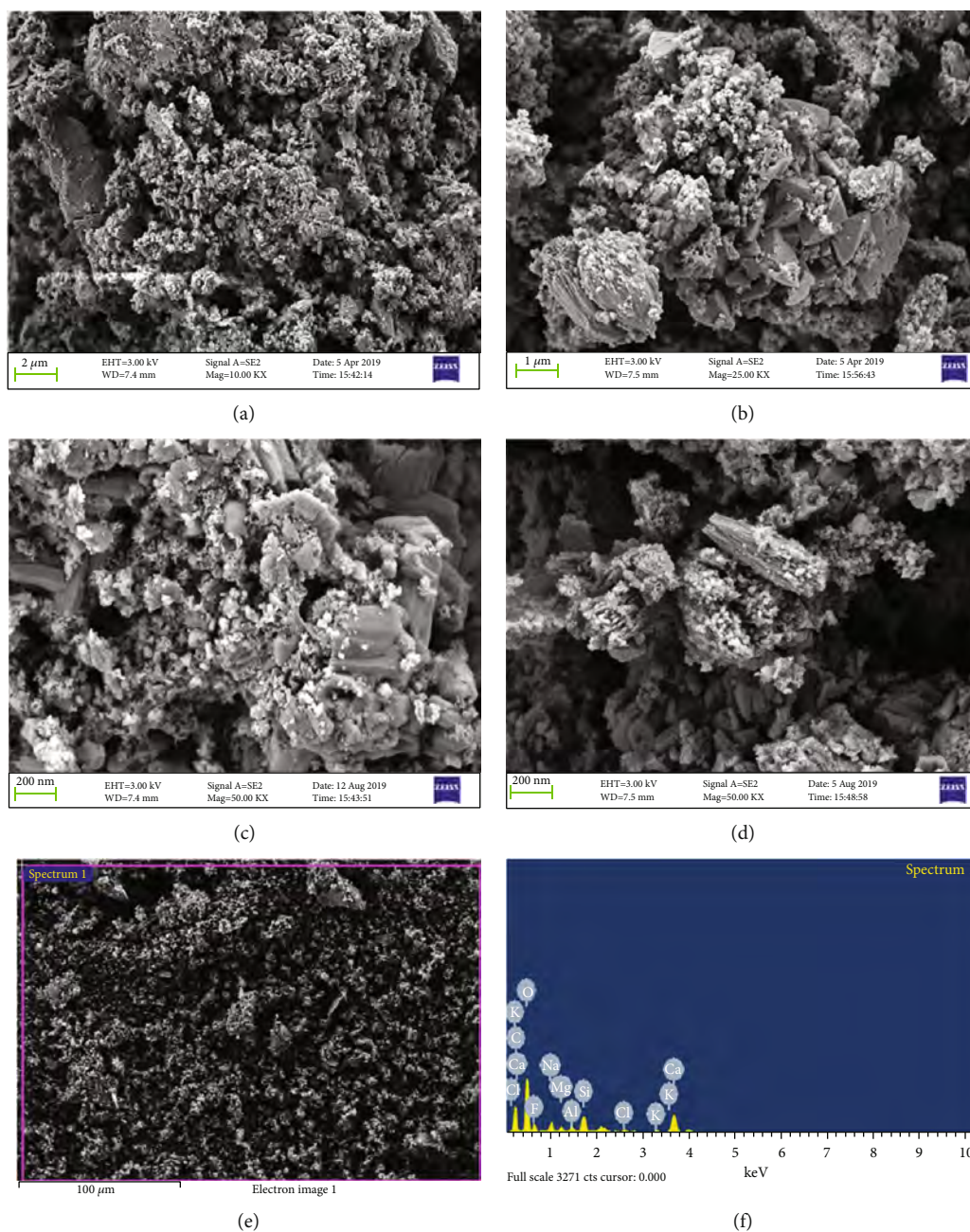


FIGURE 5: FESEM micrographs of the sintered product (a–d), EDS spot (e), and EDS spectra.

analyzed using a one-way ANOVA test with the least-significant difference test. Values of  $*p < 0.05$  were considered statistically significant.

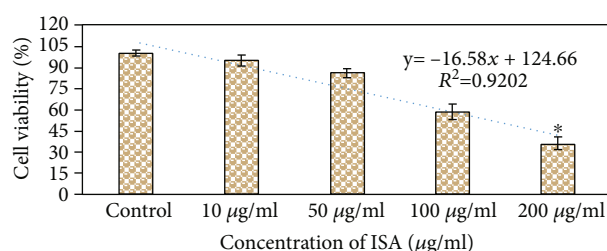
### 3. Results and Discussion

The ISA is considered hazardous waste due to the presence of heavy metals as reported earlier by Yadav et al. At the same time, it has calcium and magnesium oxides (nearly 50–56%), carbon (30%), silica (20%) alumina, and ferrous (5–8%) along with traces of other elements like Na, K, Ti, and P [11]. Some of the minerals like calcite, magnetite, silicates, and aluminates are in crystalline form, while silica is

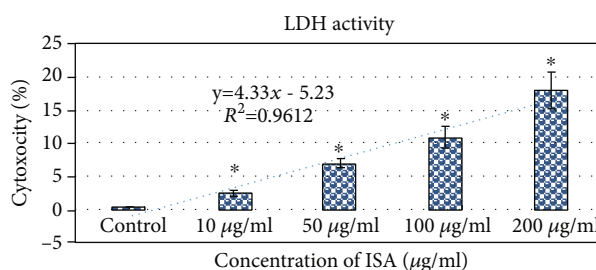
present in both glassy and amorphous forms which come from coal [11]. The crystalline material has less reactivity with the acids and bases due to their inert nature. So, the NaOH will break the crystalline structure like calcite, aluminosilicates, and glassy amorphous silica. The interaction of NaOH with Ca-rich ISA, Na will replace the Ca from the complex due to higher reactivity than Ca [12]. Further, as silica have more reactivity with NaOH so, all the aluminosilicate bonds will break and new Na-rich mineral will form in the sintered product [13, 14]. The NaOH interaction and sintering will create new pores on the surface of the sintered product so the final product will be highly porous which will enhance the adsorption process. Moreover, the ISA has

TABLE 3: Elemental analysis of ISA and ISA sintered product by EDS.

Elements	ISA (weight %)	ISA sintered product (Wt %)
C	31.28	20.18
O	41.33	37.78
Mg	1.53	1.25
Al	1.12	1.10
Si	3.09	5.41
K	1.45	0.75
Ca	20.21	20.80
F	—	8.8
Cl	—	1.04
Na	—	2.91
Total	100.00	100.00



(a)



(b)

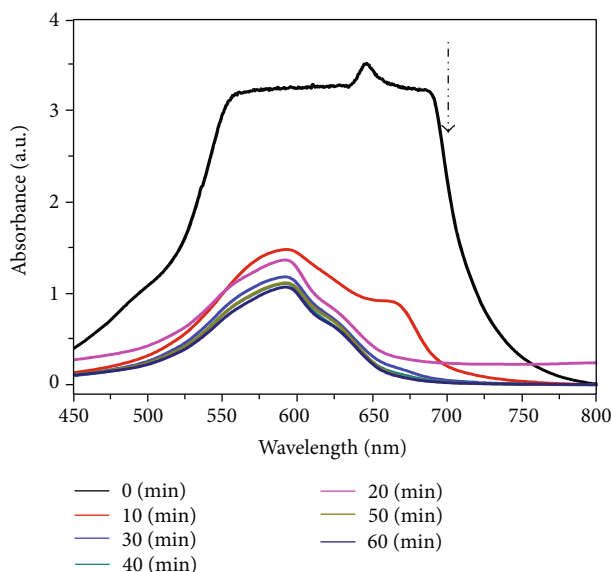
FIGURE 6: Cytotoxicity of ISA on the RTG-2 cell line for 24 h. (a) MTT assay and (b) LDH assay. Each value represents the average  $\pm$  SE of three experiments.  $n = 3$ ,  $*p < 0.5$  versus control.

FIGURE 7: Absorption spectrum representing time-dependent removal of methylene blue dye using sintered incense stick ash product.

more unburned carbon in the form of soots, chars that cannot be burned completely due to the combustion of incense sticks at a lower temperature. So, during sintering, at  $600^{\circ}\text{C}$ , most of the carbons are burned completely which will also

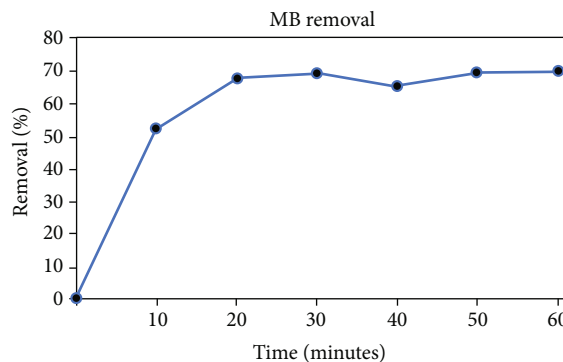


FIGURE 8: Percent removal of methylene blue dye by using sintered incense stick ash product as an adsorbent.

help in forming the porous nature of the sintered product [11].

**3.1. FTIR Analysis of ISA and ISA Sintered Product.** The typical FTIR pattern of ISA and the sintered product is shown in Figure 2. The infrared spectral data obtained for ISA shows a band near  $400\text{ cm}^{-1}$ – $700\text{ cm}^{-1}$ , which are attributed to the Fe-O, Si-O-Si, Si-Al, and Al-O-Al due to silicates, alumina. The IR absorption peak near  $750\text{ cm}^{-1}$  is assigned to Mg-OH while the band near  $900\text{ cm}^{-1}$  and  $1100\text{ cm}^{-1}$  is due to Al-OH bending vibration and silicates (Si-O-Si), respectively [15]. A weak intensity IR absorption peak observed near  $2600\text{ cm}^{-1}$  is associated with hydride vibration

TABLE 4: Dye removal percentage and adsorbent's capacity.

Time (minutes)	0	10	20	30	40	50	60
Dye removal (%)	—	52.21%	67.72%	69.05%	65.22%	69.52%	69.74%
Absorption efficiency of sintered ISA (mg/gm)	—	264	342.47	349.24	329.83	351.57	352.68

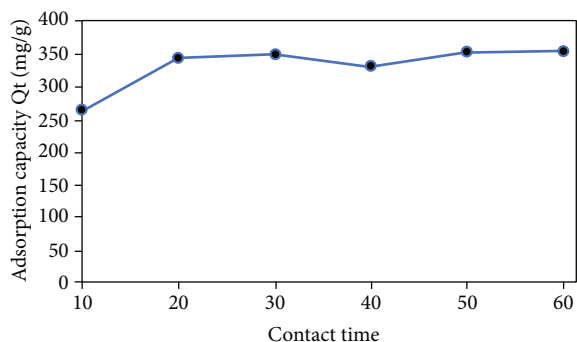


FIGURE 9: Effect of the contact time on adsorption capacity of sintered ISA for methylene blue dye.

from the silane group (Si-H). Also, the existence of C=C-C aromatic ring vibrations is being displayed by a band near  $1500\text{ cm}^{-1}$  [16]. Broadband near  $3400\text{ cm}^{-1}$  corresponds to the O-H stretch (due to the presence of water molecules in ISA) as reported by several investigators [11]. Similar observations were also reported by Yadav et al. and Jain et al. where they characterized the ISA. Jain et al. used the ISA as an economical adsorbent for the removal of Victoria blue dye from the aqueous phase without any modification [11, 17].

The ISA structure has been prominently affected due to NaOH addition. The IR spectra for sintered ISA exhibited all the characteristic peaks of ISA with slight shifts in position and intensity which confirm the interaction between the ISA and NaOH. A comparison among spectral data of raw ISA and sintered ISA provided that certain absorption peaks in ISA near  $490\text{ cm}^{-1}$ ,  $1500\text{ cm}^{-1}$ , and  $1800\text{ cm}^{-1}$  were shifted towards the higher wavenumber side suggesting that the mass of the molecule is reduced due to heating while in the sintering process. The absorption band near  $3400\text{ cm}^{-1}$  disappeared in ISA-NaOH due to the loss of water molecules during sintering. Decreased intensity of the stretching groups at  $700\text{ cm}^{-1}$  and  $900\text{ cm}^{-1}$  indicates the formation of the new group showing Na interaction with Al-O and Si-O groups.

**3.2. Phase Identification of ISA and ISA Sintered Product by XRD.** The composition and phase detection of materials is identified with the help of the XRD technique. The XRD diffractogram of ISA and sintered ISA is shown in Figure 3. The XRD pattern of ISA is semicrystalline as it shows a few intense peaks at angle  $2\theta = 20.3^\circ$ ,  $29^\circ$ , and  $42^\circ$ , while the diffraction peak at  $20.3^\circ$  is due to  $\text{SiO}_2$ . Similar observations were also obtained by Yadav et al., where they also reported calcite, magnetite, maghemite, and silicates peaks. Silica was present in both glassy amorphous and crystalline forms. The peaks at  $23^\circ$ ,  $29^\circ$ ,  $36^\circ$ , and  $48^\circ$  are due to the cal-

cite phase as a major mineral in the ISA [18], while the small peaks at  $33^\circ$  and  $35^\circ$  are due to the maghemite and magnetite in the ISA. The existence of small, broader, and overlapping reflections in the diffraction pattern of ISA indicates a low-order structure (due to amorphous carbon in ISA). The presence of carbon and silicon has been also confirmed in the FTIR results. The XRD pattern of sintered ISA shows peaks at  $2\theta = 17.3^\circ$ ,  $28^\circ$ ,  $32.8^\circ$ ,  $38^\circ$ , and  $44^\circ$ . Various peaks in sintered ISA were found to have decreased intensities. A decrease in various peak intensities shows the addition of some material that is absorbing X-rays. Additionally, the sintering process has changed the material composition as a function of temperature [18, 19].

**3.3. Morphological Analysis of ISA and ISA Sintered product by FESEM.** The surface morphology and elemental analysis of ISA were observed using FESEM and EDS. Microscopic images of ISA were obtained at low energy of 3 KeV using FE-SEM to avoid damage during the analysis process. Figures 4(a)–4(d) show the FE-SEM image of ISA at different magnification levels. FESEM images reveal that ISA is a mixture of particles having irregular shapes and sizes. The particles are agglomerated. The images show some lightly colored (carbon) and some dark-colored materials (electron-rich particles). The size of the ISA particles ranged from 100 nm to 9 microns. Similar observations were also reported by Yadav et al., for the ISA images [11].

The FESEM images (Figures 5(a)–5(e)) of sintered ISA show discrete particles having a wide range of size and highly irregular in shape. The images reveal a mixture of particles where some light-colored porous particles are placed over the surface of some large-sized dark electron-rich particles. Figures 5(c) and 5(d) show some flower-like structures. Figure 5(f) shows the elemental analysis of sintered ISA. Since there was NaOH-based alkali treatment of ISA, so, the Ca present in ISA was replaced by the Na as Na has more reactivity than Ca. When NaOH reacts with the aluminosilicates of ISA and silica, then, there is a fusion of silica, while some of the silicates will be transformed into sodium silicate after sintering.

**3.4. Elemental Analysis of ISA and ISA Sintered Product.** The elemental analysis of ISA was carried out using EDS. The results showed that the ISA sample contained elements like C, Ca, Si, Mg, Al, and Si. Carbon was found to be the principal element followed by calcium and silicon. The presence of these elements in ISA has already been confirmed with the data obtained by FTIR and XRD. The majority of elements observed in a sintered sample are C, Ca, F, Si, Na, Mg, Al, Cl, and K. The values of elements of both ISA and ISA sintered products are given in Table 3.

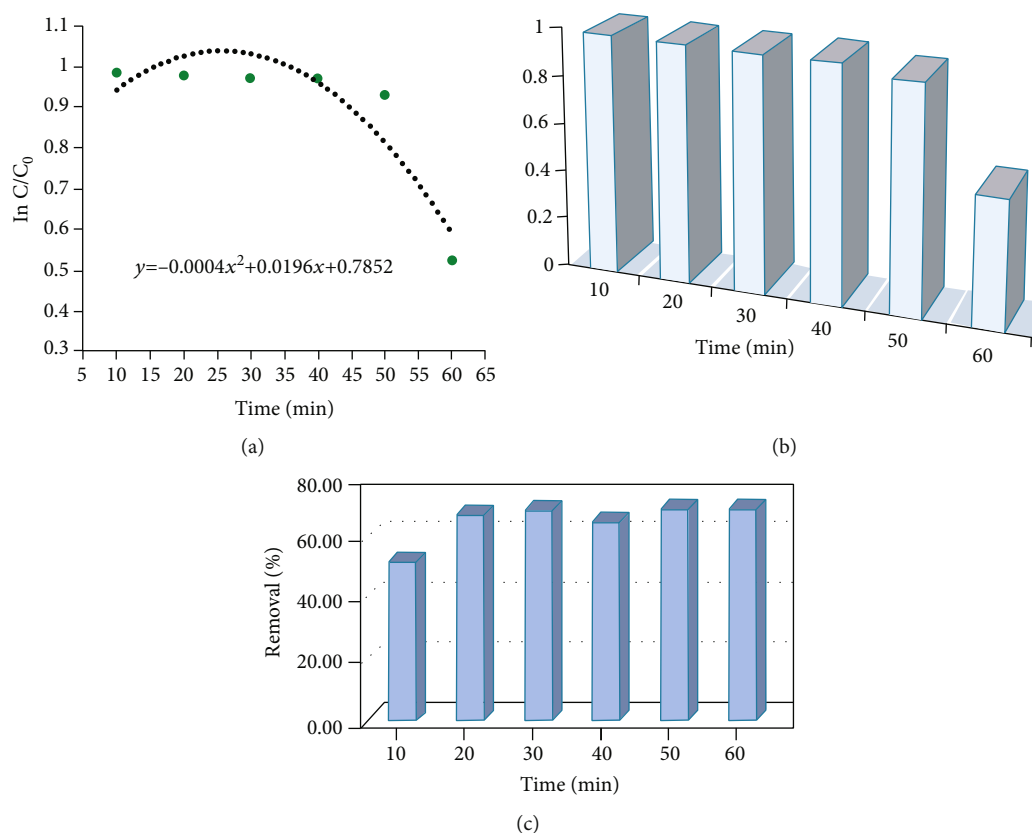


FIGURE 10: Degradation kinetics studies: (a, b) degradation rate of ISA for methylene blue dye degradation with time and (c) degradation percentage of methylene blue dye using incense stick ash.

The composition of carbon drastically decreased ( $\sim 11\%$ ) in the ISA-sintered product in comparison to the ISA, as expected due to the volatilization of organic and unburned carbon after sintering. Since the ISA is burned in open-air conditions at a low temperature, so, most of the carbon is unburned and burns completely only at the high temperature provided during sintering. There was a decrease in the O, Al, K, and Mg contents in the ISA sintered product, while the percentage of Si increased by 2.32% in the ISA-sintered product due to the breakage of aluminosilicate bond by NaOH at high temperature, and as a result, more Si were present freely in the mixture. The peaks were observed for the F, Cl, and Na in the ISA sintered product, which was initially absent in the ISA sample. Na was expected as it came from the NaOH, while during this step, chlorides might have also formed which was not observed earlier, while the high percentage of F indicates the impurity or contamination from the previous sample during EDS analysis, since there was no fluorine present in the ISA. So, this might be due to the handling error either at reaction or imaging.

**3.5. Cytotoxicity.** Cytotoxicity of a ISA sintered product on RTG-2 cell lines was measured by using MTT and LDH tests. The cytotoxicity data was represented in Figures 6(a) and 6(b). ISA induced cytotoxicity on the RTG-2 cell line in a dose-dependent manner but maximum induction of cytotoxicity was observed at  $200 \mu\text{g/mL}$  ISA (Figures 6(a) and 6(b)).

The cell viability of ISA-sintered product ( $10, 50, 100,$  and  $200 \mu\text{g/mL}$ ) was observed to be 95%, 86%, 58%, and 35.6% for 24 h in the RTG-2 cell line (Figure 6(a)). The cytotoxicity of the ISA sintered product (0, 10, 50, 100, and  $200 \mu\text{g/mL}$ ) was observed to be 0.5%, 2.5%, 7%, 10.8%, and 18.2% for 24 h in the RTG-2 cell line (Figure 6(b)).

**3.6. Dye Remediation Study.** The remediation study of MB from wastewater solution was done by using the ISA sintered product. Figure 7 shows the UV-visible spectra of the removal process for MB using sintered ISA. The MB absorption peak for MB at 664 nm vanished just after 10 minutes from the beginning point of the experiment. About 52.21% of the dye was removed within a 10-minute duration. Afterwards, the adsorption or removal process became slow and reached equilibrium after 50 minutes. The MB percent removal by the sintered ISA is shown in Figure 8. The efficiency of sintered ISA for MB adsorption was also calculated (Table 4).

**3.7. Effect of Contact Time on Dye Degradation.** Contact time is an important factor for the removal of MB dye (Figure 9). The maximum adsorption occurred during the initial 30 minutes of contact time between MB and sintered ISA due to high-concentration dye molecules [3]. The maximum adsorbent efficiency after 60 minutes of contact time was found to be  $352.68 \text{ mg/g}$ .

The kinetics of the MB dye degradation using the ISA-NaOH sintered product was investigated and shown in Figure 10. In order to investigate the degradation rate of dye molecules, we have simulated kinetics parameters followed by slandered polynomial fitting. The  $C/C_0$  values were calculated and used for evaluating the rate constant as shown in the equation in Figure 10(a). A comparative ratio of the  $C/C_0$  values with respect to time is shown in Figure 10(b) for more clearance. Furthermore, the percentage of MB degradation is calculated for the different time at a fixed amount of the used catalyst (20 mg) and is shown in Figure 10(c). However, the inorganic elements such as Si, Fe, and Mg in ISA (confirmed by EDX and XRD) could occur in the form of metal oxides in the ISA. These inorganic species felicitate an efficient adsorption tendency and promote the degradation rate for organic dye compounds. In the present scenario, the ISA-NaOH sintered product shown an effective degradation rate as it is used as a cost-effective and eco-friendly adsorbent. This material could be further explored in degradation Chemistry of the organic aromatic substance including various dye molecules and derivatives [20, 21].

Earlier, Jain et al. reported the remediation of Victoria Blue dye with an efficiency of 80% by using whole ISA collected from temples. Moreover, Yadav et al. also reported the synthesis of Ca-rich zeolites whose size was 200 nm in width and 700 nm in length which was later on utilized for the removal of alkali metals (Ba, Ca, Mg, Mn, and Al) and heavy metals like Cu, Cd, Cr, Co, Ni, Pb, and Zn from aqueous solutions. The removal percentage of heavy metals were varying from 20% to 70% within two hours only while concentration of Pb reached below the detection level of ICP-OES as it was initially present in very less concentration. The rod to cuboidal-shaped zeolite particles was also highly porous like the NaOH-treated sintered product.

#### 4. Conclusions

The utilization of incense stick ash waste-derived value-added product as an economical adsorbent opens a new material in the field of adsorption science and environmental cleanup. The present work utilized the waste incense stick ash after transforming the nature of the material for remediation of methylene blue. The incense stick ash sintered products developed after NaOH treatment and calcination were analyzed, and it was found that the particle is flower shaped, micron sized, i.e., 100 nm to 9 microns, and highly porous. The porosity is due to the presence of the huge amount of unburned carbon which after calcination got volatilized and made the incense stick ash sintered product more porous which was evidenced by the FESEM. The increase in the size of the sintered product could also be due to the calcination at high temperature where the particles got fused with NaOH. Due to the porous nature of the incense stick ash sintered product, it was assessed for the removal of methylene blue dye in the batch adsorption study. The removal percentage of methylene blue dye from the wastewater was up to 70% within one hour only. The present research thus confirmed that sintered ISA is a novel and eco-

nomical adsorbent for remediation of methylene blue dye. Such value-added material developed from the waste ISA could act as a potential, economical, and efficient adsorbent for the remediation of dye and other inorganic and organic pollutants from the water solutions.

#### Data Availability

The datasets used and analyzed during the current study are available from the corresponding author upon reasonable request.

#### Consent

All authors have read and approved the manuscript to be published.

#### Conflicts of Interest

The authors declare that there is no conflict of interest.

#### Acknowledgments

This work was funded by the researchers supporting project number (RSP-2021/165), King Saud University, Riyadh, Saudi Arabia.

#### References

- [1] R. K. Chandini, R. Kumar, and P. Om, "The impact of chemical fertilizers on our environment and ecosystem," *Research Trends in Environmental Sciences*, vol. 35, pp. 69–86, 2019.
- [2] G. Samchetshabam, A. Hussan, T. Gon Choudhury, S. Gita, P. Soholar, and A. Hussan, "Impact of textile dyes waste on aquatic environments and its treatment," *Environment & Ecology*, vol. 35, pp. 2349–2353, 2017.
- [3] Y. Kuang, X. Zhang, and S. Zhou, "Adsorption of methylene blue in water onto activated carbon by surfactant modification," *Water*, vol. 12, no. 2, p. 587, 2020.
- [4] S. Alkaykh, A. Mbarek, and E. E. Ali-Shattle, "Photocatalytic degradation of methylene blue dye in aqueous solution by MnTiO<sub>3</sub> nanoparticles under sunlight irradiation," *Heliyon*, vol. 6, no. 4, p. e03663, 2020.
- [5] S. De Gisi, G. Lofrano, M. Grassi, and M. Notarnicola, "Characteristics and adsorption capacities of low-cost sorbents for wastewater treatment: a review," *Sustainable Materials and Technologies*, vol. 9, pp. 10–40, 2016.
- [6] A. A. Yaqoob, T. Parveen, K. Umar, and M. N. Mohamad Ibrahim, "Role of nanomaterials in the treatment of wastewater: a review," *Water*, vol. 12, no. 2, p. 495, 2020.
- [7] M. E. A. El-sayed, "Nanoadsorbents for water and wastewater remediation," *Science of the Total Environment*, vol. 739, p. 139903, 2020.
- [8] S. Homaeigohar, "The nanosized dye adsorbents for water treatment," *Nanomaterials (Basel)*, vol. 10, no. 2, p. 43, 2020.
- [9] V. K. Yadav, "The current scenario of Indian incense sticks market and their impact on the Indian economy," *Indian Journal of Pure & Applied Biosciences*, vol. 8, no. 3, pp. 627–636, 2020.

- [10] T.-C. Lin, G. Krishnaswamy, and D. S. Chi, "Incense smoke: clinical, structural and molecular effects on airway disease," *Clinical and Molecular Allergy*, vol. 6, no. 1, p. 3, 2008.
- [11] V. K. Yadav, G. Gnanamoorthy, M. M. S. Cabral-Pinto et al., "Variations and similarities in structural, chemical, and elemental properties on the ashes derived from the coal due to their combustion in open and controlled manner," *Environmental Science and Pollution Research*, vol. 28, no. 25, 2021.
- [12] L. Liu and A. Corma, "Metal catalysts for heterogeneous catalysis: from single atoms to nanoclusters and nanoparticles," *Chemical Reviews*, vol. 118, no. 10, pp. 4981–5079, 2018.
- [13] M. Barreto Santos, J. De Brito, and A. Santos Silva, "A review on alkali-silica reaction evolution in recycled aggregate concrete," *Materials (Basel)*, vol. 13, no. 11, p. 20, 2020.
- [14] F. Hagemans, W. Vlug, C. Raffaelli, A. van Blaaderen, and A. Imhof, "Sculpting silica colloids by etching particles with nonuniform compositions," *Chemistry of Materials*, vol. 29, no. 7, pp. 3304–3313, 2017.
- [15] Y. Yin, H. Yin, Z. Wu et al., "Characterization of coals and coal ashes with high Si content using combined second-derivative infrared spectroscopy and Raman spectroscopy," *Crystals*, vol. 9, no. 10, p. 513, 2019.
- [16] J. Zhuang, M. Li, Y. Pu, A. Ragauskas, and C. Yoo, "Observation of potential contaminants in processed biomass using Fourier transform infrared spectroscopy," *Applied Sciences*, vol. 10, no. 12, p. 4345, 2020.
- [17] S. N. Jain, S. R. Tamboli, D. S. Sutar, V. N. Mawal, A. A. Shaikh, and A. A. Prajapati, "Incense stick ash as a novel and sustainable adsorbent for sequestration of Victoria blue from aqueous phase," *Sustainable Chemistry and Pharmacy*, vol. 15, p. 100199, 2020.
- [18] H. Ferral-Pérez, M. Galicia-García, B. Alvarado-Tenorio, A. Izaguirre-Pompa, and M. Aguirre-Ramírez, "Novel method to achieve crystallinity of calcite by *Bacillus subtilis* in coupled and non-coupled calcium-carbon sources," *AMB Express*, vol. 10, no. 1, p. doi:10.1186/s13568-020-01111-6, 2020.
- [19] D. I. Sapparuddin, N. A. N. Hisham, S. A. Aziz et al., "Effect of sintering temperature on the crystal growth, microstructure and mechanical strength of foam glass-ceramic from waste materials," *Journal of Materials Research and Technology*, vol. 9, no. 3, pp. 5640–5647, 2020.
- [20] S. Kitouni and A. Harabi, "Sintering and mechanical properties of porcelains prepared from algerian raw materials," *Cerâmica*, vol. 57, no. 344, pp. 453–460, 2011.
- [21] M. Yeleuov, C. Seidl, T. Temirgaliyeva et al., "Modified activated graphene-based carbon electrodes from rice husk for supercapacitor applications," *Energies*, vol. 13, no. 18, p. 4943, 2020.